DC Grids

20NRM03 DC grids

https://dc-grids.nl

Proposed test waveforms for DC electricity meter testing

Eidgenössisches Institut für Metrologie METAS
Istituto Nazionale di Ricerca Metrologica
Università degli studi della Campania Luigi Vanvitelli
VSL B.V.

31 May 2024

This project has received funding from the EMPIR programme co-financed by the Participating States and from the European Union's Horizon 2020 research and innovation programme.

EMPIR EURAMET
The EMPIR initiative is co-funded by the European Union's Horizon 2020 research and innovation programme and the EMPIR Participating States

DC Grids

Contents

This project has received funding from the EMPIR programme co-financed by the Participating States and from the European Union's Horizon 2020 research and innovation programme.

EMPIR EURAMET

The EMPIR initiative is co-funded by the European Union's Horizon 2020 research and innovation programme and the EMPIR Participating States

Scope

In this industry guide, a set of significant test waveforms for DC electricity meter testing is presented. The selection has been driven by two main criteria: on one side, the consistency (when applicable) with similar tests performed on AC electricity meters; on the other side, the analysis of real-world waveforms as acquired in different DC microgrid installations. Based on these considerations, this industry guide represents a first attempt to identify the most significant power quality issues that may affect DC electricity meters, and discusses their potential consequences in terms of measurement error and uncertainty.

1 DC microgrid scenario

The project *DC grids* addresses the challenges and open issues of power and energy metering in Low Voltage DC (LVDC) microgrids [1]. It is thus important to keep in mind the specific application scenario, where the measurement devices will be deployed.

Indeed, modern power systems are experiencing a rapid transformation due to the ever-increasing penetration of renewable energy sources (RES) and distributed generation. Most of these resources are characterized by DC outputs, and dedicated power converters are needed to interconnect them to the AC bulk grid. Such a paradigm allows for a drastic reduction of the power system's carbon footprint, but on the other hand, is the root cause of many operational challenges such as the loss of rotational inertia and the degradation of power quality.

For these reasons, when possible, it is advised to build DC microgrids, where energy production and consumption do not need any intermediate transformation stage. This is particularly useful when the energy demand profile can be predicted with sufficient accuracy in advance. Typical examples are railway stations and airports where the energy demand follows repetitive and deterministic patterns. Other promising application scenarios are represented by parking lots or public lighting infrastructures.

Unfortunately, though, the normative framework for DC metering is still intended for traditional DC sources and do not consider the possible uncertainty contributions related to the peculiar RES functioning and the disturbances that may be injected at the point of interconnection with the AC bulk grid.

2 Definitions and references

In this guide, we refer to DC electricity static meters, whose voltage and current levels are limited to 1000 V and 800 A, respectively. From a normative point of view, the reference standards in terms of metrological performance are:

- IEC 62052-11:2020 (Edition 2.0) *"Electricity metering equipment - General requirements, tests and test conditions - Part 11: Metering equipment"*, June 2020 [2].
- IEC 62053-41:2021 (Edition 1.0) *"Electricity metering equipment - Particular requirements - Part 41: Static meters for DC energy (classes 0,5 and 1)"*, June 2021 [3].

In this regard, it is worth noticing that a static meter is defined as a meter in which current and voltages act on solid state (electronic) elements to produce an output proportional to the energy to be measured. Typically, in AC electricity meter, the energy measurement is output in terms of a pulsated signal, either optical (metrological led) or electrical (digital switching output). In both these cases, the energy measurement is expressed in terms of number of pulses, according to the specific meter constant (typically, pulse per kWh). Nevertheless, the same information could be also stored in digital registers, that may be accessible either from the meter display or via a dedicated user interface.

Measurand definition

A DC electricity meter is meant to measure DC power and energy. More precisely, DC power is defined as the product of voltage and current mean values, while DC energy is its integral as a function of time [2].

It is worth noticing that - in a pure DC context - mean and root-mean-square (RMS) values are exactly coincident. Consequently, DC active and apparent power are equivalent quantities. In real-world operating conditions, though, voltage and current signals may be affected by spurious components. In first approximation, these components can be divided into two main categories:

- wide-band noise, that can be modelled as zero-mean and statistically uncorrelated random variable. As such, its effect on mean value computation is negligible, whereas it may introduce significant errors in the RMS computation.
- ripple and fluctuations, that can be modelled as the combination of a finite series of sinusoidal components. In this case, the computation of voltage and current mean values depends on the ratio between the sinusoidal period and the averaging interval.

Given a meter that applies the DC power and energy definitions as per [2], both categories of interfering components may introduce significant errors. A straightforward solution may be represented by a low pass filtering stage [4], but the choice of the filter parameters is not so immediate and depends on the expected operating conditions.

Averaging interval

In defining DC power, the IEC-62052-11:2021 does not specify either the sampling rate or the duration of the averaging interval. For instance, in this regard, the EN 50470-4:2023 states that frequencies up to 10 Hz shall be considered as part of the measurement signal and the averaging interval shall be long enough to minimize the effect of AC power components [5].

In the AC scenario, most measuring and averaging intervals are defined as integer multiples of a rated cycle or half-cycle of the fundamental component rated period, i.e. 20 ms. A clear example in this sense is given by the different aggregation intervals employed by Power Quality Instruments (PQIs, or briefly PQ meters) according to the IEC 6100-4-30:2021 [6]: 10 ms, 200 ms, 3 s, 10 s, etc.

In the DC scenario, instead, there is no clear reference in terms of synchronization or time intervals. Even in the reporting of the measured results there is no clear rule: some meters report a new energy value each second, some others produce aggregated values over five minutes in accordance with many Supervisory Control and Data Acquisition (SCADA) applications [7].

Based on all the previous considerations, in the *DC grids* project, we perform power and energy measurements based on non-overlapped intervals of 200 ms. On one side, this value is in line with the traditional PQ meters' functioning. In this way, it would be easier to compare measurements coming from different devices, even on two different parts of the network (one in the DC microgrid, one in the interconnected AC grid). On the other side, such an averaging interval represents a good trade-off between tracking sudden variations of the DC levels and rejecting spurious injections from components whose period is (nearly) an integer multiple of 200 ms, i.e. AC frequencies multiple of 5 Hz.

Sampling rate

In a similar way, also the selection of the meter sampling rate depends on the kind of phenomena it is expected to accurately detect. Some on-field applications rely on waveform recorders, and thus adopt sampling rates in the order of hundreds of kHz. This proves to be extremely beneficial for fault location

or spectral analysis [8,9]. On the other hand, purely metering applications focus on the DC component and a reduced bandwidth (e.g., 10 Hz), therefore can employ sampling frequencies in the order of tens of kHz [10]. In practice, the choice of the most suitable sampling rate shall account for several aspects: the noise level, the variation range as well as the stability of the DC levels. A faster sampling rate allows for spreading the wide-band noise on a wider spectrum and thus reduces its interference on the final measurement, but this comes at the cost of a poorer vertical resolution (e.g., number of bits). Based on the expected operating scenario and performance target, it is possible to identify the most suitable setup.

3 Test waveform selection

Based on theoretical and experimental investigations, it is possible to identify the operating conditions and power system events that are more likely to affect DC meter functioning. For this analysis, we considered two main information sources. First, the analysis of the test conditions adopted in the AC case. Second, the evaluation of the most recurrent power quality events, as recorded in experimental measurement campaigns in DC microgrids.

At the end of this process, we identified three main classes of test waveforms:

1. harmonic distortion
2. voltage dips and swells
3. ripple and modulation patterns

In the following paragraph, we are going to provide a short description of each class, and to discuss its significance with respect to DC meter functioning.

3.1 Harmonic distortion

In a DC scenario, the concept of harmonic may sound improper. Nevertheless, it is reasonable to expect that the acquired signal may be corrupted by harmonic injections of power converters in the grid.

The test is meant to characterize the frequency response of the DC meter in the presence of AC power components with different magnitudes and frequencies. It is important to underline that the AC components represent influence quantities and - as such - should be completely rejected by the DC meter.

To this end, the test waveforms of voltage $u(t)$ and current $i(t)$ consist of the superposition of a DC component and a single AC component at the time:

$$\begin{aligned} u(t) &= DC_U + \frac{A_U}{\sqrt{(2)}} \cdot \cos(2\pi f_U \cdot t + \varphi_U) \\ i(t) &= DC_I + \frac{A_I}{\sqrt{(2)}} \cdot \cos(2\pi f_I \cdot t + \varphi_I) \\ t &= n \cdot T_s, \quad n \in \mathcal{Z}^+ \end{aligned} \tag{1}$$

where the subscripts U and I refer to the voltage and current waveforms, respectively. Both test waveforms are expressed as a function of the time variable t, defined as a finite series of consecutive integer multiples of the sampling period T_s.

The DC component values should be varied within the range of interest. In the *DC grids* project, voltage and current were upper limited to 1000 V and 800 A, respectively. To span the entire variation range, it is suggested to repeat test (2) by varying the DC values according to a logarithmic rule:

$$DC_x = (0.01, 0.02, 0.05, 0.10, 0.20, 0.50, 1.00) \cdot DC_x^{max} \tag{2}$$

where x indicates either voltage or current, and DC_x^{max} the corresponding full-scale DC value.
As regards the AC component, the variation ranges for magnitude and frequency are as follows:

$$A_x = (0.01, 0.02, 0.05, 0.10) \cdot DC_x \tag{3}$$

$$f_x = (0.1, 1, 10, 100, 150, 300, 1000, 10000, 10000)\,\mathrm{Hz} \tag{4}$$

where the magnitude is expressed as a function of the DC value. On the other hand, the frequency spans a very wide range. Frequencies lower than or equal to 10 Hz are supposed to be included in the measurand definition. As such, they are meant to evaluate the meter response to slow DC variations. Higher frequencies, instead, shall be considered spurious distortions and be thus suitably rejected.

In this guide, the proposed variation range arrives in the order of hundreds of kHz (i.e., the so-called supra-harmonic range). If f_x exceeds the meter Nyquist rate (i.e., half of the sampling rate), the test may lose its metrological relevance. Nonetheless, it could be useful to validate the anti-aliasing filter of the meter analog front-end.

As regards the phase difference between voltage and current waveforms, it is allowed to adopt random and statistically independent values. Indeed, the AC components shall be considered influence quantities. The only exception is represented by the test waveforms whose frequency is lower than or equal to 10 Hz. In that case, it may be interesting to evaluate the meter response in two conditions:

- voltage and current angle coincide such that $\cos(\varphi_U - \varphi_I) = 1$
- current in quadrature with voltage such that $\cos(\varphi_U - \varphi_I) = 1$

The first one corresponds to a pure AC active power condition and should be included in the DC power computation. Conversely, the second one corresponds to a pure AC reactive power and should produce negligible variations in the DC power computation.

Fig. 1 and 2 present two examples of test waveforms, as analyzed in the time and frequency domain on the left and right sides, respectively. In both cases, the test waveforms have been normalized by the selected DC component value, such that it is possible to express the vertical axis in *per unit* (pu). For this analysis, we consider a sampling rate of 100 kHz and an averaging interval of 0.2 s. Consequently, the spectral representation spans from 0 Hz (DC) to 50 kHz (Nyquist rate), with a resolution of 5 Hz. The combined effect of quantization and measurement noise is approximated by means of an uncorrelated white Gaussian noise with a Signal-to-Noise Ratio (SNR) of 80 dB. The AC component magnitude is 1 % of the DC one, while the frequency is set equal to 1 Hz and 1 kHz in Fig. 1 and 2, respectively.

In the first case, the AC component frequency is included within the 10-Hz bandwidth introduced by [5]. Indeed, it is interesting to observe in Fig. 1(a) how DC and AC components are not easily discriminated. Their combination results in a slowly varying DC offset. Similar considerations hold for the spectral representation in Fig. 1(b): DC and AC components merge in a single larger lobe.

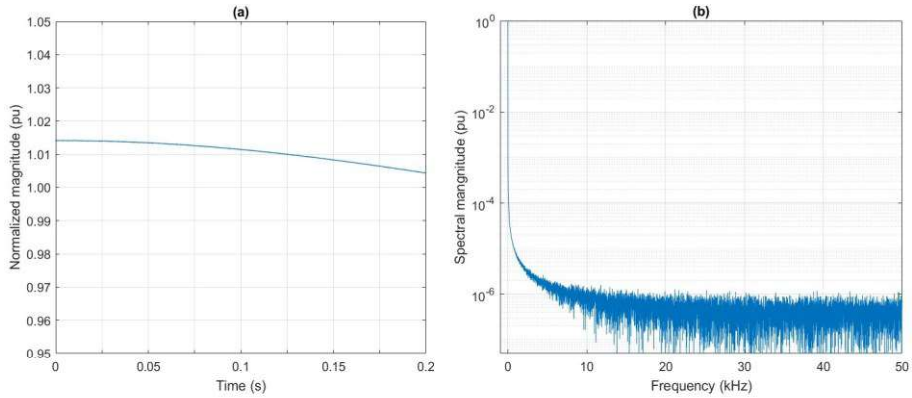

Figure 1: Time and frequency domain representation of a test waveform corrupted by a 1-Hz sinusoidal component in (a) and (b), respectively.

In the second case, instead, the AC component shall be considered an influence quantity. As shown in Fig. 2(a), in the time domain AC and DC components are totally uncorrelated. In Fig. 2(b), the spectral representation presents a white noise uniformly spread all over the spectrum, and two single-bin components: the DC component at 0 Hz, and the AC component at 1 kHz.

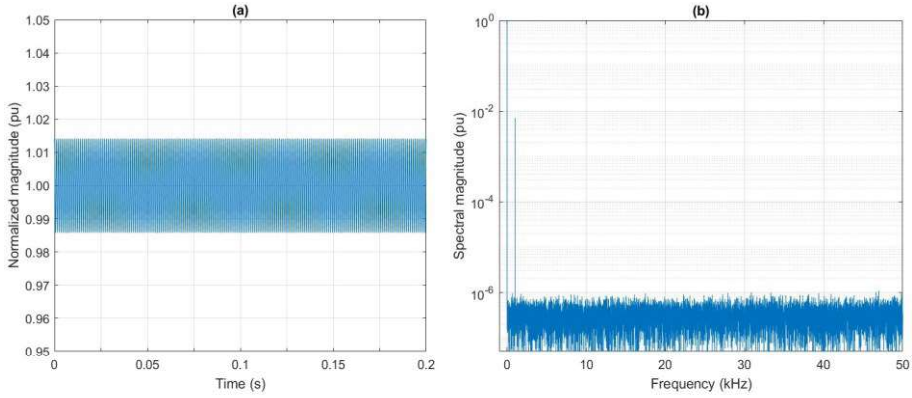

Figure 2: Time and frequency domain representation of a test waveform corrupted by a 1-kHz sinusoidal component in (a) and (b), respectively.

3.2 Voltage dips and swells

Voltage dips and swells are phenomena that take place frequently in DC microgrids. From a mathematical point of view, they can be represented by sudden variations of the DC level, and can be identified in terms of two parameters, namely their duration and depth. By taking as reference the PQI standard [6], dips and swells shall have a minimum duration and depth of 40 ms and 20 %, respectively.

To span a realistic range of situations, this industrial guide suggests considering test waveforms derived from the following set of parameters:

- dip/swell duration: 40 ms or 250 ms
- dip/swell depth: 20 % or 30 %

The events can be repeated periodically with a frequency of 1 Hz, for an overall duration of 1 minute (or an entire reporting period of the DC meter, if larger than 1 minute). The DC level is typically kept to its nominal value, but it could be also varied in a limited interval (e.g., $DC_x = (0.5, 0.75, 1.0)DC_x^{max}$).

For example, Fig. 3 represents two dips, with the same depth (-20 %) and different duration (40 ms and 250 ms). For the sake of clarity, the time axis has a duration of 1 s, and both events are triggered at its midpoint. The sampling rate is equal to 100 kHz, and the SNR is equal to 80 dB.

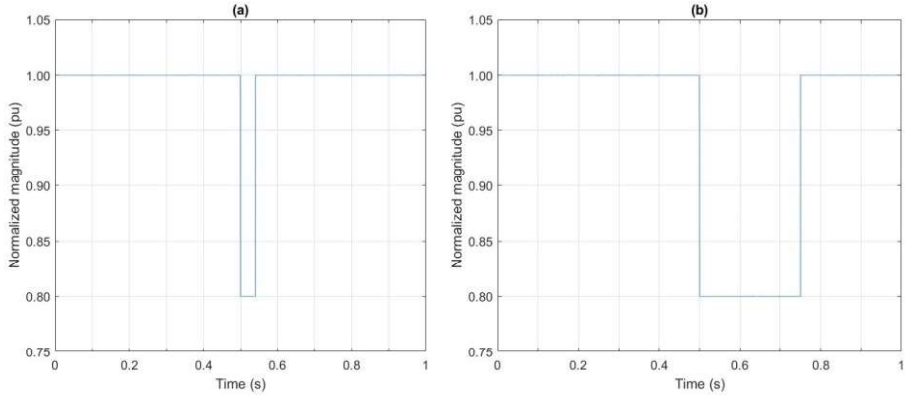

Figure 3: Voltage 20-% dip events with a duration of 40 and 250 ms in (a) and (b), respectively.

In such test waveforms the variations of DC level are instantaneous and follow a square-wave pattern. As a consequence, it is possible to define in a deterministic way their effect on the computation of DC voltage, and thus on the computation of DC power (and energy).

In this sense, a simple example could be beneficial in understanding the effect of a voltage dip in the computation of DC power. For the sake of simplicity, let us assume both voltage and current DC levels are equal to 1 pu. As a consequence, also the DC power value is equal to 1 W. The voltage waveform is affected by a dip whose depth and duration are set equal to 20 % and 40 ms, respectively. In the following, we report the DC voltage (and, thus, DC power) errors as a function of the averaging interval[1]:

$$\begin{aligned} &\text{interval}: 0.2\ \text{s} \qquad \Delta DC_U = -4.0\ \% \\ &\text{interval}: 0.5\ \text{s} \qquad \Delta DC_U = -1.6\ \% \\ &\text{interval}: 1.0\ \text{s} \qquad \Delta DC_U = -0.8\ \% \end{aligned} \tag{5}$$

If - instead - the objective is to test the robustness of the DC meter in the presence of sudden and irregular voltage changes, it is preferred to adopt the same test waveforms presented in the IEC 625862:2021 [11][2]. For the sake of completeness, Fig. 4 presents the reference voltage dip and swell profiles in (a) and (b), respectively. Two inset graphs allow for a better understanding of the peculiar voltage profile of each event. It should be noticed how both events are extremely rapid, namely a duration of about 10 ms. The DC level is not constant neither before, during nor after the event. For these reasons, it is hard to define a deterministic formula for the DC voltage and DC power expected errors. Nonetheless, it is interesting to observe whether (and to which degree) the DC meter is affected by similar events.

[1] In this test, we assume the voltage dip is entirely contained in the considered averaging interval.

[2]The voltage swell and dip are taken from Fig. 5 and 6 of the IEC 62586-2:2021.

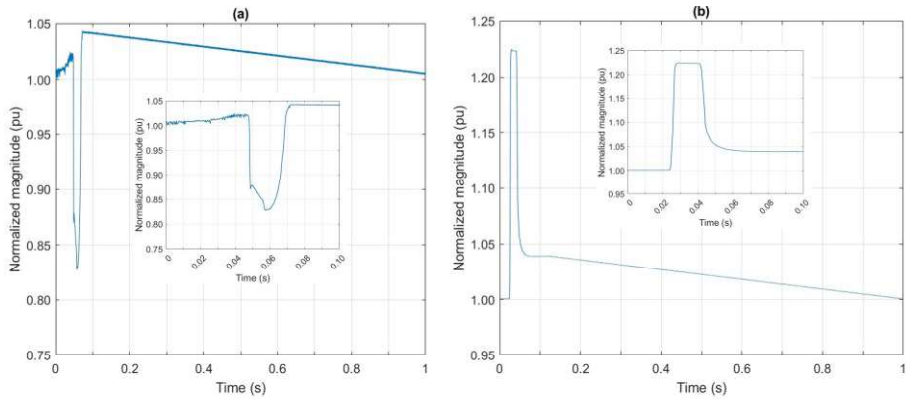

Figure 4: Voltage dip and swell as derived from the IEC 62586-2:2021 [11] in (a) and (b), respectively. The insets provide a closer look at the dip and swell profiles in the first 10 ms of the event.

3.3 Ripple and modulation patterns

In real-world scenarios, the most common disturbance is represented by voltage and current ripple [12]. This is typically due to the alternating voltage component of the voltage on the DC side of a power converter. From a mathematical point of view, ripples can be approximated as square or triangular modulations, centered around the DC component value [13].

In the time domain, such test waveforms can be expressed as follows:

$$\begin{aligned} \text{square}: u(t) &= DC_U + SQ_U \cdot \left[\text{sgn}\left(\cos\left(\frac{2\pi t}{T_{SQ}}\right)\right) - 0.5\right] \\ \text{triangle}: u(t) &= DC_U + TR_U \cdot \left[\frac{2}{\pi}\arcsin\left(\sin\left(\frac{2\pi t}{T_{TR}}\right)\right) - 0.5\right] \end{aligned} \quad (6)$$

where sgn, cos, arcsin, and sin indicate the sign, cosine, arcsine, and sine function, respectively. The parameters SQ_U and TR_U indicate the peak-to-peak amplitude of the square- and triangular-wave modulation, while T_{SQ} and T_{TR} are the corresponding periods. Similar formulations can be applied also to the current test waveforms.

In the frequency domain, both test waveforms are characterized by an infinite series of sinusoidal components, namely the modulation frequency and its odd harmonics each one decaying according to a linear function of their harmonic order. For this test, modulation amplitude and frequency can be set in a similar way as per the harmonic test in Section 3.1. This would allow us to evaluate the actual bandwidth of the DC meter in the presence of wide-band disturbances. Being centered around the DC value, their effect in terms of DC power should be negligible. However, the low pass filtering effect inherent in any meter analog front-end may produce some distortions in the acquired signal and thus result in errors or larger variability.

In this context, Fig. 5 and 6 present two examples of square- and triangular-wave modulations, respectively. More precisely, the left plot shows the time-domain profile of the test waveform, while the right plot shows the corresponding spectral representation. In both cases, the modulation peak-to-peak amplitude is set to 10 % of the DC component, while the modulation frequency is equal to 300 Hz (consistently with typical switching frequency values of power converters). As expected, the test waveform spectra consist of an infinite set of evenly spaced components, namely the odd harmonics of the modulation frequency up to the Nyquist rate.

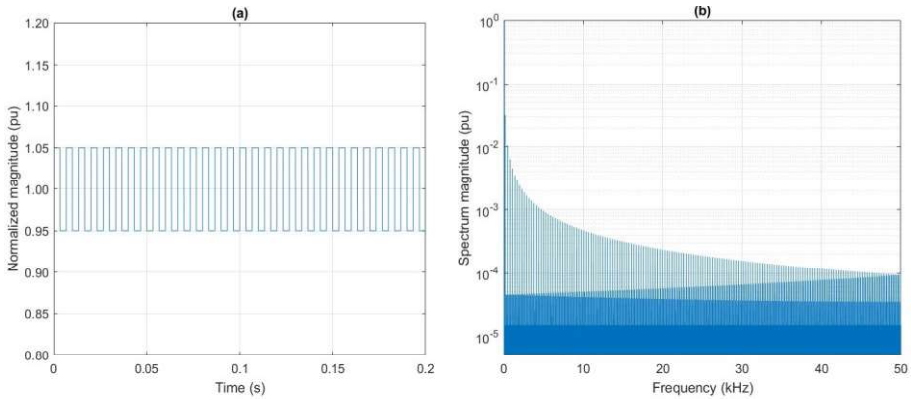

Figure 5: Time- and frequency-domain representation of a DC component affected by square-wave ripple in (a) and (b), respectively.

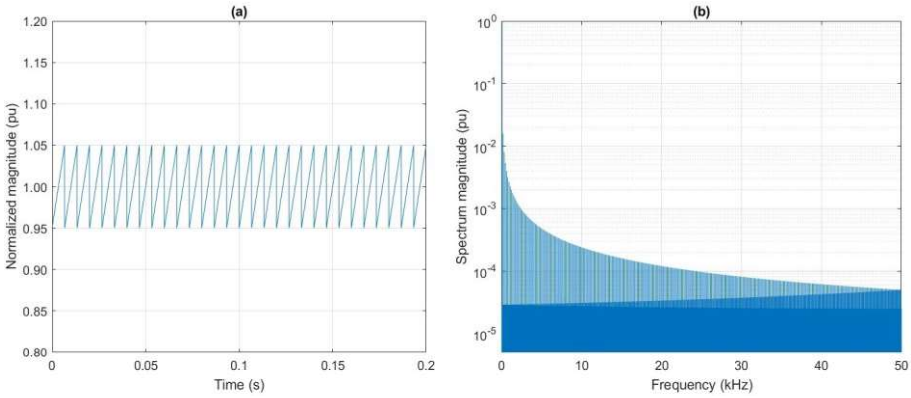

Figure 6: Time- and frequency-domain representation of a DC component affected by triangular-wave ripple in (a) and (b), respectively.

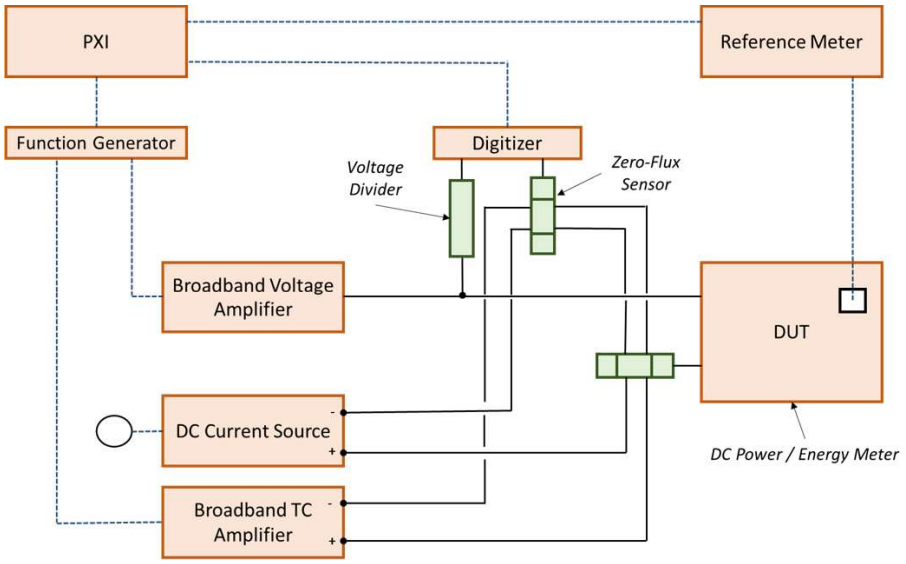

Figure 7: Block scheme of the METAS reference system for DC power and energy. The VSL system has a very similar architecture.

4 Test waveform generation

The generation of the selected test waveforms requires the development of *ad-hoc* reference systems, capable of reproducing both pure and distorted DC levels. In this regard, Fig. 7 presents a simplified block scheme of the DC power reference system, as developed at the Federal Institute of Metrology METAS, in Bern, Switzerland [14]. A similar system was designed and validated at VSL in Delft, the Netherlands [15].

As with many other electrical metrology applications, the system relies on a generation and re-acquisition principle. In this way, it is possible to define the reference values of the test waveforms supplied to the Device Under Test (DUT), in this case the DC meter.

An industrial controller, namely a NI PXI 1042Q (National Instruments, Austin, TX) is responsible for setting and triggering a Function Generator (FGEN) and a Digitizer (DIG) board. The FGEN reproduces a low-voltage version of the voltage and current test waveforms. In the voltage case, the waveform is sent to a broadband voltage amplifier, whose output range and bandwidth are incompatible with maximum DC level (1 kV) and AC frequency (150 kHz). In the current case, DC and AC components are generated separately. A DC current source outputs a DC current up to 800 A, whereas a transconductance amplifier allows for reproducing AC components up to 100 A and 150 kHz. To merge DC and AC components, there exist several approaches [13–16], but the easiest and safest solution is to exploit a zero-flux DC Current Transformer (DCCT), where both DC and AC conductor are inserted. The DCCT inherent functioning merges the two signals and produces a single output signal (as scaled by the transformation factor).

Voltage and current test waveforms are now ready to be supplied to the DUT. The resulting power and energy can be accessed either through the internal meter register or - in a simpler way - by means of a switching output (optical or electrical).

The same test waveforms are simultaneously re-acquired by the NI PXI by means of a well-calibrated voltage divider and DCCT. The acquired waveforms are then processed via a non-linear fit routine to extract the DC reference value for both current and voltage.

Finally, based on this information and on the meter output, a power comparator or a reference power meter can calculate the DC meter error. To be sure that both the reference system and the DUT observe the same signal, it is possible to introduce a controllable switch on the voltage channel and perform an energy dosage measurement: the closure and re-opening of the switch represent the starting of ending point of the energy integration interval [17].

5 Preliminary experimental results

To evaluate the actual feasibility of the previous considerations, a measurement campaign has been conducted to evaluate the effect of distorted DC waveforms on commercial meters [18].

For this analysis, we compared a reference DC meter developed at METAS [10] versus a commercial meter, i.e. DZG DC Meter GSH01 (Deutsche Zahlergesellschaft, Hamburg, Germany). The commercial device is certified as class-B accuracy, with maximum voltage and current levels of 1500 V and 650 A, respectively.

For this test, we consider DC voltage and current of 750 V and 500 A, respectively. A single AC component is superposed simultaneously on both voltage and current signals. The AC magnitude is 75 V and 100 A, while the frequency varies between 0.1 Hz and 300 Hz. Each test has a duration of 10 minutes, and the DC power estimates are collected and compared against the reference value as given by the METAS reference system. To this end, the METAS reference meter updates its power estimates every 200 ms. For the sake of comparability, we measured the electrical switching output of the DC meter and retrieved the equivalent power estimate with the same reporting rate (i.e. 5 measurements per second).

In this context, Fig. 8(a) shows the absolute errors in DC power as measured by the METAS reference meter and the commercial DUT as blue crosses and violet squares, respectively. In a similar way, Fig. 8(b) shows the corresponding expanded uncertainty (with a cover factor k = 2), as obtained by combining the reference system uncertainty (around 150 ppm) and the Type A uncertainty of the meter results. Both meters show an evident performance degradation for AC frequencies below 10 Hz. The power errors exceed even 1 %, and the corresponding uncertainty achieves a worst-case level of 15 %.

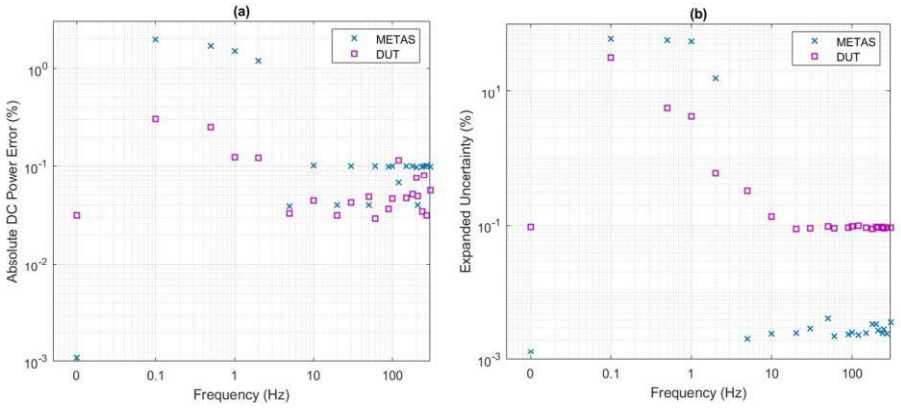

Figure 8: Absolute DC power error (a) and corresponding expanded uncertainty (b) for the METAS DC reference meter and the commercial DUT in blue and violet, respectively.

These results prove the importance of testing DC meters in distorted conditions. The lack of clear indications in terms of sampling rate, averaging interval length, and pass-bandwidth are limiting factors for the widespread deployment of this technology in modern DC microgrids. The test waveforms included in this industry guide represent a useful tool to characterize the meter in more challenging and realistic conditions and allow for a pre-validation of their functioning in on-field applications.

Bibliography

[1] 20NRM03, “Dc grids: Standardisation of measurements for dc electricity grids a joint research project with the european metrology programme for innovation and research,” https://dc-grids.nl/.

[2] IEC-62052-11, “Electricity metering equipment - general requirements, tests and test conditions part 11: Metering equipment,” IEC, Tech. Rep., 2020.

[3] IEC-62053-41, “Electricity metering equipment - particular requirements - part 41: Static meters for dc energy (classes 0,5 and 1),” IEC, Tech. Rep., 2021.

[4] G. Frigo and F. Costa, “DC power metering in low-voltage microgrids: Definitional and methodological issues,” in *2023 4th International Conference on Smart Grid Metrology (SMAGRIMET)*, 2023, pp. 1–6.

[5] EN-50470-4, “Electricity metering equipment - part 4: Particular requirements - static meters for dc active energy (class indexes a, b and c),” European Committee for Electrotechnical Standardization, Tech. Rep., 2023.

[6] IEC-61000-4-30:2015+AMD1:2021, “Electromagnetic compatibility (emc) - part 4-30: Testing and measurement techniques - power quality measurement methods,” IEC, Tech. Rep., 2021.

[7] IEC-TS-62361-102:2018, “Power systems management and associated information exchange - interoperability in the long term - part 102: Cim - iec 61850 harmonization,” IEC, Tech. Rep., 2018.

[8] H. E. van den Brom, R. van Leeuwen, G. Maroulis, S. Shah, and L. Mackay, “Power quality measurement results for a configurable urban low-voltage dc microgrid,” *Energies*, vol. 16, no. 12, 2023. [Online]. Available: https://www.mdpi.com/1996-1073/16/12/4623

[9] M. A. Oliván, J. J. Pérez-Aragüés, and J. J. Melero, “A high-frequency digitiser system for real-time analysis of dc grids with dc and ac power quality triggering,” *Applied Sciences*, vol. 13, no. 6, 2023. [Online]. Available: https://www.mdpi.com/2076-3417/13/6/3871

[10] G. Frigo and M. Agustoni, “Development of a transfer standard for dc power quality reference systems,” in *2022 IEEE 12th International Workshop on Applied Measurements for Power Systems (AMPS)*, 2022, pp. 1–6.

[11] IEC-62586-2:2017+AMD1:2021, “Power quality measurement in power supply systems - part 2: Functional tests and uncertainty requirements,” IEC, Tech. Rep., 2021.

[12] G. Cipolletta, A. D. Femine, D. Gallo, C. Landi, and M. Luiso, “Considerations on voltage ripple assessment in dc power network,” in *2022 IEEE 12th International Workshop on Applied Measurements for Power Systems (AMPS)*, 2022, pp. 1–6.

[13] M. Blaz, J. Langemann, M. Schmidt, and C. Leicht, “Setup for testing energy meters with disturbed dc signals occurring in dc charging stations,” in *2023 IEEE 13th International Workshop on Applied Measurements for Power Systems (AMPS)*, 2023, pp. 1–6.

[14] G. Frigo and J. Braun, “Measurement setup for a dc power reference for electricity meter calibration,” in *2022 Int. Conf. on Harmonics & Quality of Power (ICHQP)*, 2022, pp. 1–5.

[15] H. van den Brom, Z. Marais, and R. van Leeuwen, “Testing of DC Electricity Meters with Broadband Conducted Electromagnetic Disturbances”, in *2022 Int. Conf. on Harmonics & Quality of Power (ICHQP)*, Naples, Italy, May 2022.

[16] D. Giordano, D. Signorino, A. D. Femine, and D. Gallo, “Setup for the calibration of current measuring systems under dc signals affected by ripple,” in *2023 IEEE 13th International Workshop on Applied Measurements for Power Systems (AMPS)*, 2023, pp. 1–6.

[17] C. Mester, “Dc active electrical energy meters: Accuracy tests,” in *2022 IEEE 12th International Workshop on Applied Measurements for Power Systems (AMPS)*, 2022, pp. 1–6.

[18] G. Frigo, D. Giordano, and D. Signorino, “Inter-laboratory comparison of transfer standard for dc power measurements in nominal and distorted conditions,” in *2024 Conference on Precision Electromagnetic Measurements (CPEM 2024)*, 2024, pp. 1–2.